Supporting Information

Reversible Structural Transformations and Color-Tunable Emissions in Organic Manganese Halides

Yu-Hang Liu[a,b], Yi-Fan Wu[a], Li-Juan Feng[a], Rui-Rui Zhao[a], Shan-Xiao Wang[a], Ming-Ming Zhang[a], Dan-Yang Wang[a], Xiang-Wen Kong[a]*, Xiao-Wu Lei[a]*

[a] School of Chemistry, Chemical Engineer and Materials, Jining University, Qufu, Shandong, 273155, P. R. China

[a] School of Chemistry and Chemical Engineering, Qufu Normal University, Qufu, Shandong, 273165, P. R. China

Corresponding author: Xiang-Wen Kong, Xiao-Wu Lei

E-mail address: kxw2021@126. com, xwlei_jnu@163.com

Experimental Section

Materials. The chemical materials and organic reagents were purchased from Aladdin Chemical Company, including $MnCl_4 \cdot H_2O$ (99.99%), hydrochloric acid (HCl, 37%), 1,4-Dimethylpiperazine (DMPZ, 99 %), ethanol (99%) and *n*-Propanol (99%). All the above materials were directly used without any further purification or other physical processes.

Synthesis of [DMPZ]$MnCl_4$ (1). Mixture of $MnCl_4 \cdot H_2O$ (10 mmol, 0.20 g) and DMPZ (10 mmol, 0.11 g) dissolved in the solution containing HCl (1 mL), ethanol (5 mL) and *n*-propanol (2 mL). The solution was stirred magnetically for 1 hour under slight heating (~40 ℃) to obtain clear solution. The mixed solution was then sealed in a 25 mL glass vial and reacted at 80 ℃ for 7 days. After cooling to room temperature, green emissive crystals were obtained, which were determined to be [DMPZ]$MnCl_4$ ($C_6N_2H_{16}MnCl_4$) by single crystal X-ray diffraction. The crystals were then washed repeatedly with ethanol three times and dried in vacuum. Anal. Calcd. for $C_6N_2H_{16}MnCl_4$: C, 23.03%; H, 5.15%; N, 8.95%; found: C, 22.91%; H, 5.45%; N, 8.92%.

Synthesis of $[DMPZ]_4(MnCl_6)(MnCl_4)_2 \cdot (H_2O)_2$ (2). Single crystal of compound **2** was prepared in the same chemical environment as that of **1**. After the formation of compound **1**, the mother liquid containing the single crystals of **1** were left silently at room temperature. After 15 days, all the green-emissive crystals of **1** transform to red-emissive crystals, which were determined to be $[DMPZ]_4(MnCl_6)(MnCl_4)_2 \cdot (H_2O)_2$ ($C_{24}H_{64}Cl_{14}Mn_3N_8O_2$) based on single crystal X-ray diffraction. The crystals were washed three times with ethanol and dried at room temperature. Anal. Calcd. for $C_{24}H_{64}Cl_{14}Mn_3N_8O_2$: C, 24.89%; H, 5.57%; N, 9.68%; O, 2.76%; found: C, 24.96%; H, 5.24%; N, 9.44%, O, 2.76%.

Single-crystal X-ray crystallography. Single-crystal data for [DMPZ]$MnCl_4$ and $[DMPZ]_4(MnCl_6)(MnCl_4)_2 \cdot (H_2O)_2$ were collected at room temperature by using a Bruker Apex-II CCD diffractometer with Cu-K_α radiation (λ = 1.5378 Å) at room temperature. The crystal structures were solved by direct method. Refinement was carried out on the basis of F^2 using the Olex2 program. All non-hydrogen atoms were refined with anisotropic thermal parameters, whereas the hydrogen atoms of organic

molecules were positioned isotropically. The structure refinement parameters for $[DMPZ]MnCl_4$ and $[DMPZ]_4(MnCl_6)(MnCl_4)_2\cdot(H_2O)_2$ are summarized in Table S1 and S4, and the important bond parameters are listed in Tables S2-4 and S5-7.

Powder X-ray diffraction. Powder X-ray diffraction (PXRD) analysis was carried out on a Bruker D8 advanced powder X-ray diffractometer, Cu-K_α radiation at 40 kV and 40 mA current. Scans were performed at room temperature over an angular range of 5-60° (2θ) in steps of 5 °/min. The simulated PXRD data were calculated from single crystal data in the Mercury software.

Common Characterizations. Thermogravimetric analysis (TGA) was carried out on a Mettler TGA/SDTA 851 thermal analyser in the temperature range of 30 - 800 °C. A PE Lambda 900 UV-vis spectrophotometer was used to collect solid UV-vis absorption spectra in the range of 200 - 800nm using barium sulphate as the reference standard.

PL characterization. Photoluminescence (PL) spectroscopy was performed on an Edinburgh FLS980 fluorescence spectrometer (Edinburgh Instruments, Livingston, Scotland, UK). The PLQYs were acquired by adding an integrating sphere in FLS980 fluorescence spectrometer, using Xe lamp (450 W) to generate a monochromatic light source with excitation power of 600 $\mu W/cm^2$, and then were calculated through the formula: $\eta_{QE} = I_S/(E_R - E_S)$, where I_S represents the luminescence emission spectrum of the sample, E_R is the spectrum of the excitation light from the empty integrating sphere (without the sample), and E_S is the excitation spectrum of the excited sample. Time-resolved decay data were obtained using a fluorescence spectrometer of a picosecond pulsed semiconductor laser. The average life was obtained by exponential fitting.

The Calculations of Tanabe-Sugano (T-S) Matrices. The crystal field D_q, Racah B parameters and tree correction α were obtained using the modified energy terms derived by Tanabe and Sugano as follows:

$$6S \rightarrow {}^4A_1;\ {}^4E({}^4G) = 10B + 5C + 20\alpha \quad (1)$$

$$6S \rightarrow {}^4E({}^4D) = 17B + 5C + 6\alpha \quad (2)$$

$$6S \rightarrow {}^4T_2({}^4D) = 13B + 5C + 8\alpha \quad (3)$$

$$6S \rightarrow {}^4T_2(4G) = -10Dq + 18B + 6C - (26B^2/10Dq) + 22\alpha \quad (4)$$

Calculated results: D_q = 1232, B = 1781, C = 881 and α = 47 for $[DMPZ]MnCl_4$ and D_q = 869, B = 908, C = 3430 and α = -157 for $[DMPZ]_4(MnCl_6)(MnCl_4)_2 \cdot (H_2O)_2$.

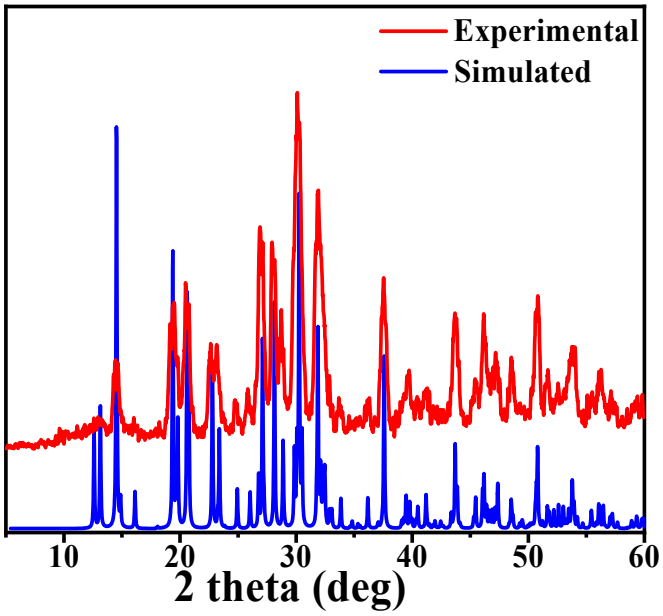

Fig. S1. The simulated and experimental PXRD patterns of $[DMPZ]MnCl_4$.

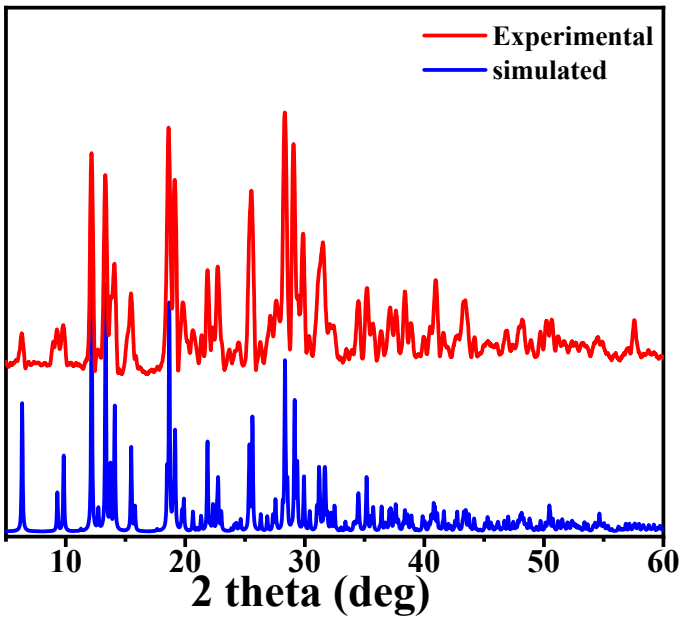

Fig. S2. The simulated and experimental PXRD patterns of $[DMPZ]_4(MnCl_6)(MnCl_4)_2 \cdot (H_2O)_2$.

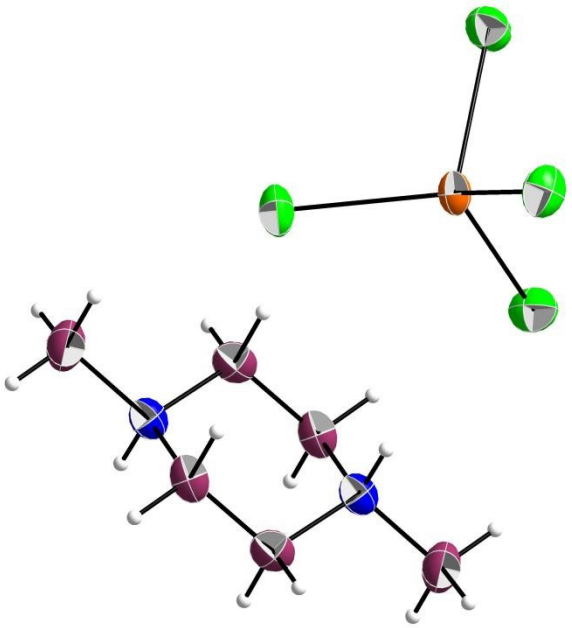

Fig. S3. ORTEP for the single crystals of $[DMPZ]MnCl_4$.

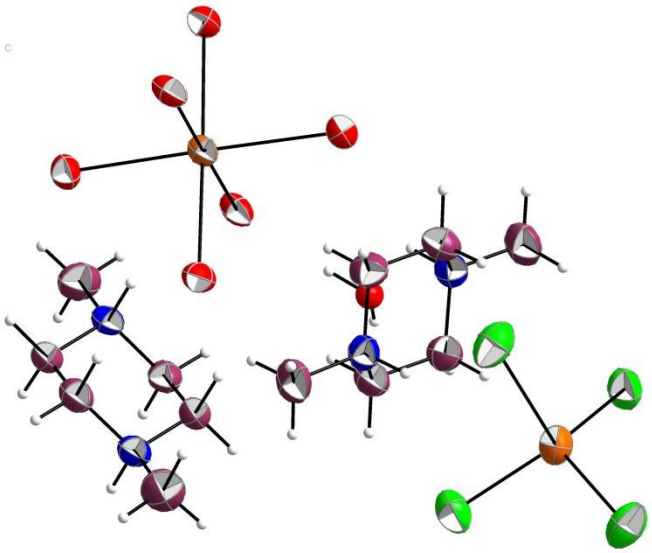

Fig. S4. ORTEP for the single crystals of $[DMPZ]_4(MnCl_6)(MnCl_4)_2 \cdot (H_2O)_2$.

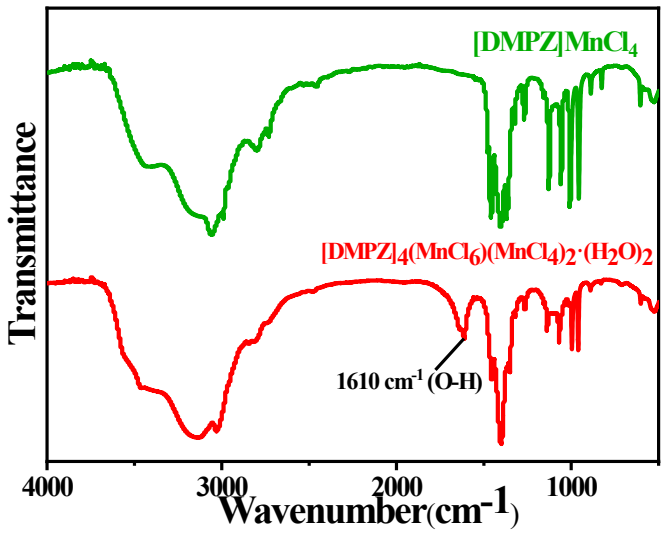

Fig. S5 . The infrared spectra of $[DMPZ]MnCl_4$ (green) and $[DMPZ]_4(MnCl_6)(MnCl_4)_2\cdot(H_2O)_2$ (red).

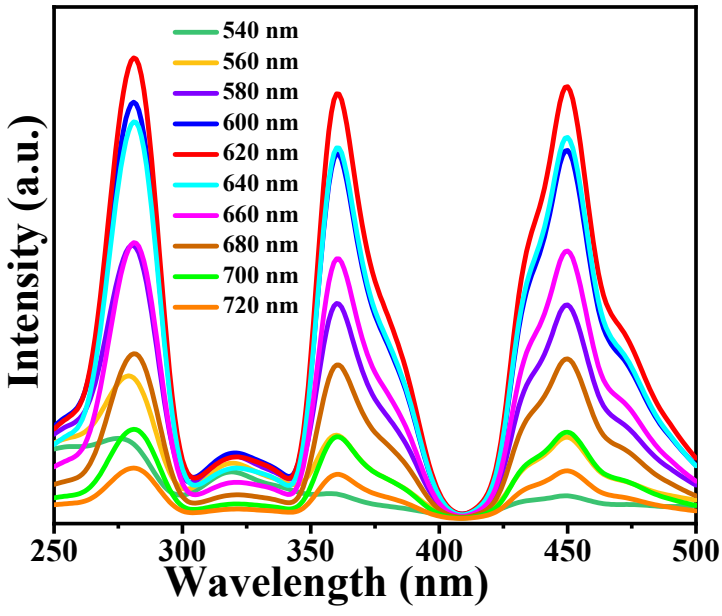

(a)

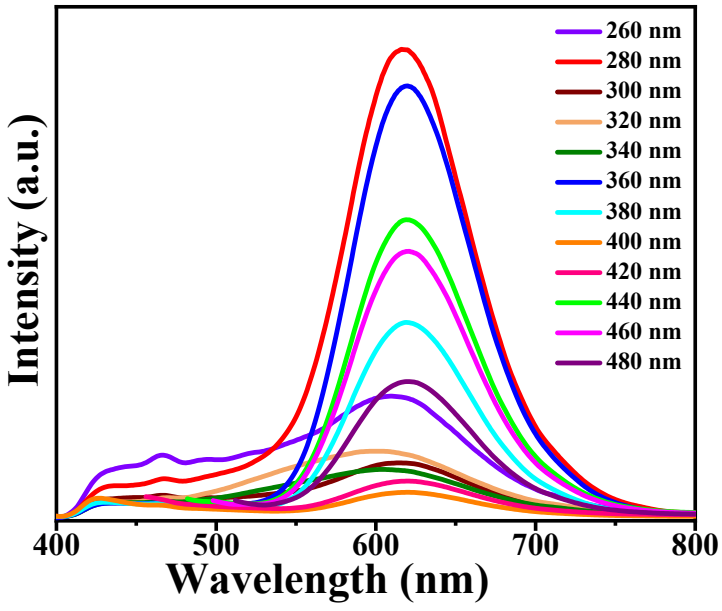

(b)

Fig. S6. The excitation wavelength dependent PL emission spectra (a) and the emission wavelength dependent PL excitation spectra (b) of [DMPZ]$MnCl_4$.

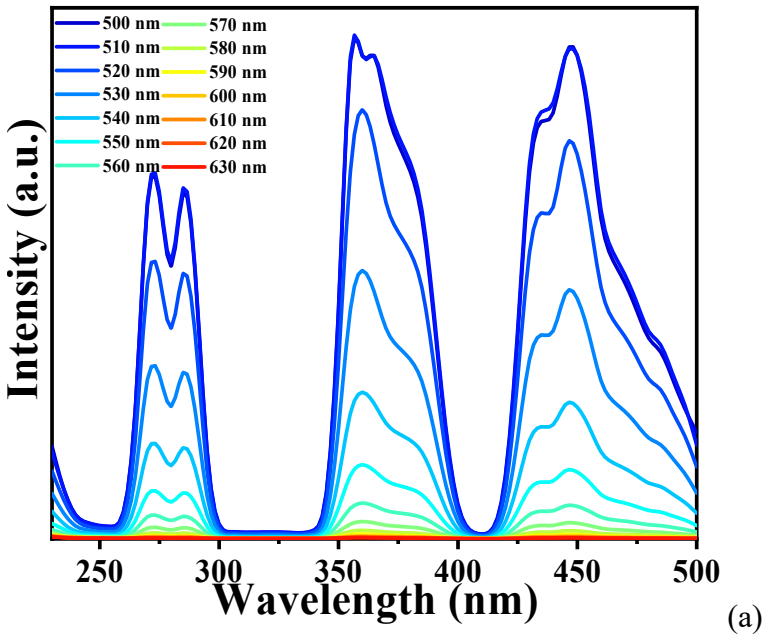

(a)

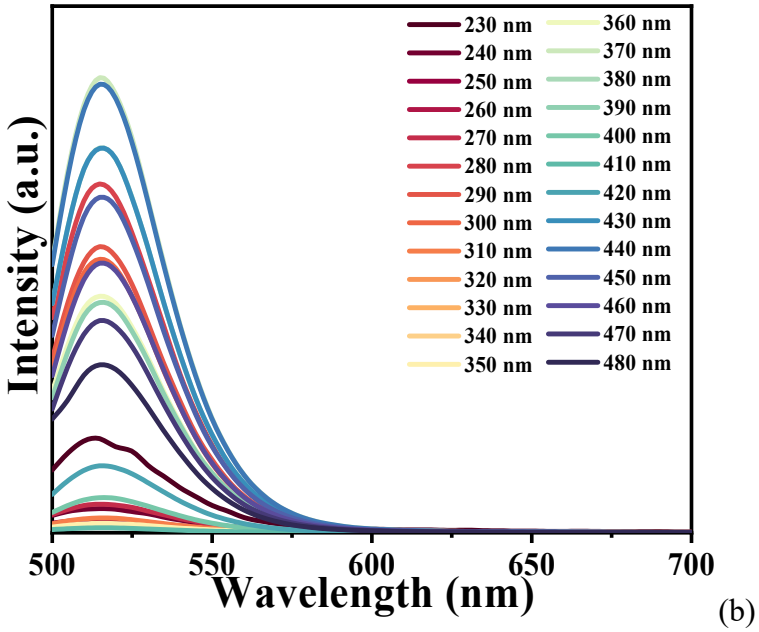

(b)

Fig. S7. The excitation wavelength dependent PL emission spectra (a) and the emission wavelength dependent PL excitation spectra (b) of $[DMPZ]_4(MnCl_6)(MnCl_4)_2 \cdot (H_2O)_2$.

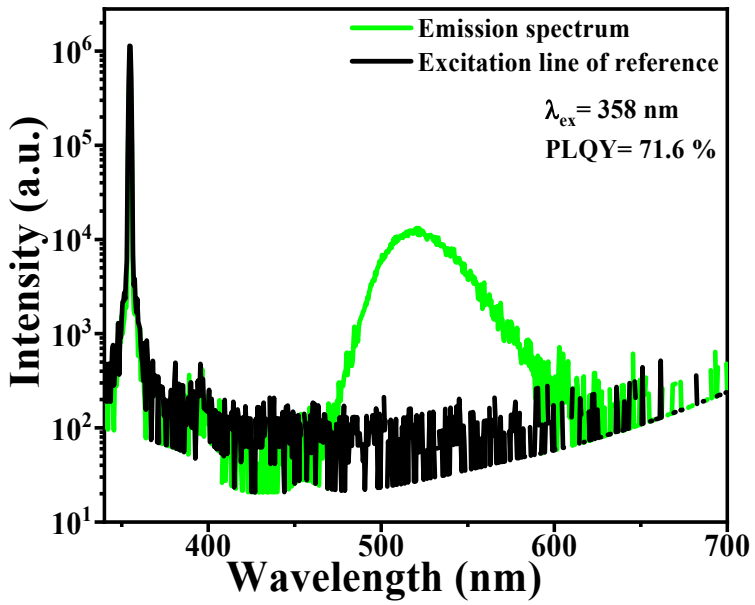

Fig. S8. The PLQY absorption spectrum of $[DMPZ]MnCl_4$ under 358 nm UV excitation.

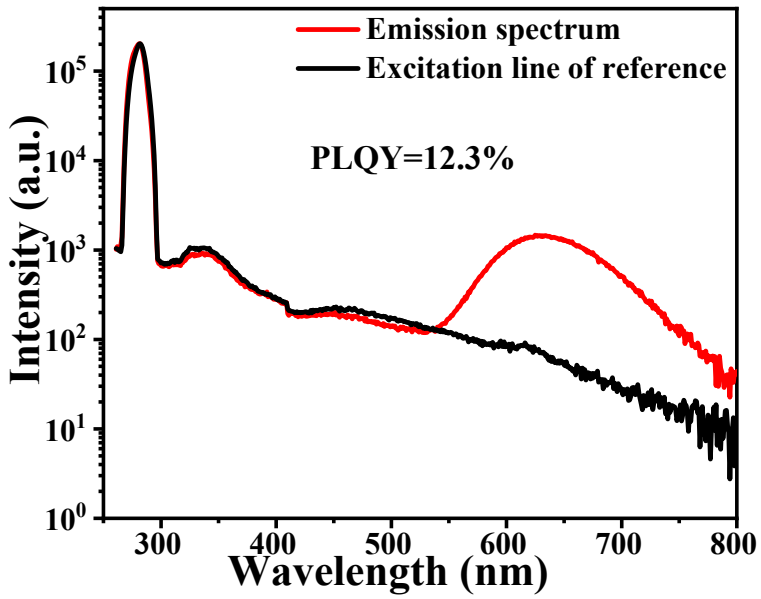

Fig. S9. The PLQY absorption spectrum of $[DMPZ]_4(MnCl_6)(MnCl_4)_2\cdot(H_2O)_2$ under 361 nm UV excitation.

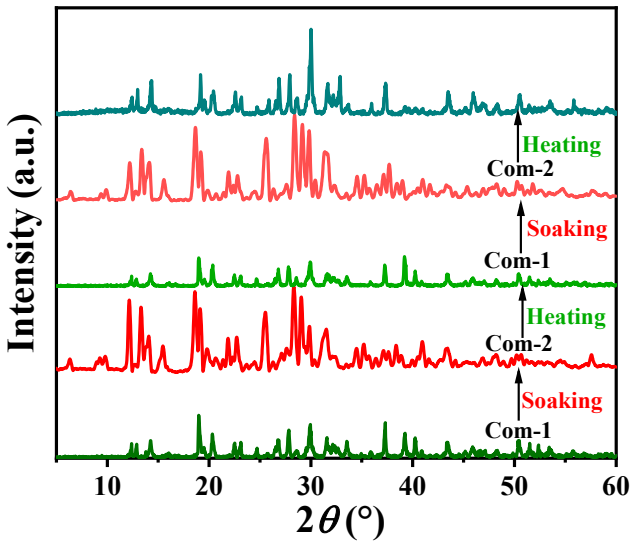

Fig. S10. PXRD patterns in the transformation between compounds **1** and **2**.

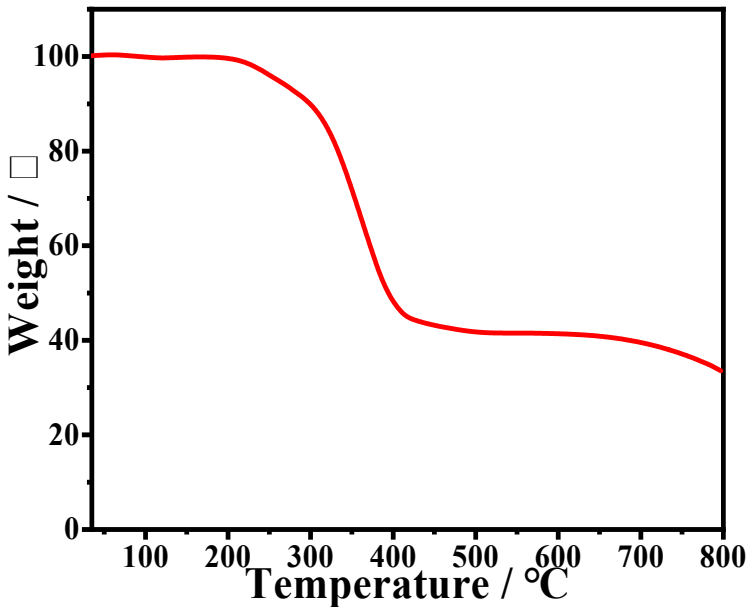

Fig. S11. The thermogravimetric analysis (TGA) curve for [DMPZ]$MnCl_4$.

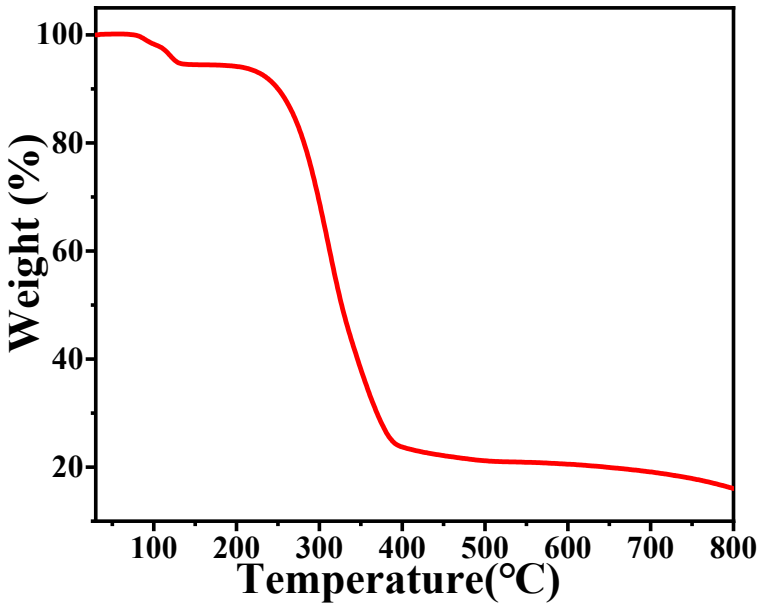

Fig. S12. The thermogravimetric analysis (TGA) curve for $[DMPZ]_4(MnCl_6)(MnCl_4)_2 \cdot (H_2O)_2$.

Table S1. Summary of PL emission switching in 0D metal halides.

Com-1			Com-2			Stimulus	Ref.
Molecular formula	λ_{em} (nm)	Emission color	Molecular formula	λ_{em} (nm)	Emission color		
$Cs_3Cu_2I_5$	445	Blue	$CsCu_2I_3$	555	Yellow	H_2O	1
$Cs_2InBr_5 \cdot H_2O$	695	Red	$Cs_3In_2Br_9$	-	Yellow	H_2O	2
$[Bzmim]_3SbCl_6$	525	Green	$[Bzmim]_2SbCl_5$	600	Red	Heat	3
$(C_4NOH_{10})_5 Mn_2Cl_9 \cdot C_2H_5OH$	620	Red	$(C_4NOH_{10})_2 MnCl_4$	520	Green	C_2H_5OH	4
$C_6N_2H_{16}MnBr_4$	548	Green	$C_6N_2H_{16}MnBr_4 (H_2O)_2$	-	No emission	H_2O	5
$[PP14]_2[PbBr_4]$	470	Blue	$[PP14]_9[PbBr_4]_2 [Pb_3Br_{11}]$	500	Green	Heat	6
α-$Gua_3Cu_2I_5$	472	Blue	β-$Gua_3Cu_2I_5$	534	Yellow-Green	Heat	7
$(PhPi)_2SbCl_7 \cdot xH_2O$	708	Red	$(PhPi)_2SbCl_7$-S	578	Yellow	Heat and acetone	8
$CsMnCl_3$-$(H_2O)_2$	618	Red	Cs_3MnCl_5	521	Green	DMF or DMAC	9
$CsMnBr_3$	600	Red	Cs_3MnBr_5	520	Green	Isopropanol	10
α-$[Bmmim]_2SbCl_5$	575	Yellow	*β*-$[Bmmim]_2 SbCl_5$	615	Orange	Inter-contacting	11

Table S2. Crystal Data and Structural Refinements for [DMPZ]$MnCl_4$.

Compound	[DMPZ]$MnCl_4$
chemical formula	$C_6N_2H_{16}MnCl_4$
fw	312.95
Space group	*P*21/*m*
a/Å	6.1254(9)
*b*Å	14.520(2)
c/Å	6.9482(10)
α/°	90.00
β/°	90.437(5)
γ/°	90.00
V(Å^3)	617.97(16)
Dcalcd (g·cm^{-3})	1.682
Temp (K)	298
μ (mm^{-1})	1.893
F (000)	318
Reflections collected	8373
Unique reflections	1587
GOF on F^2	1.065
[a]R_1,wR_2 ($I > 2\sigma(I)$)	0.0189/0.0450
[b]R_1,wR_2 (all data)	0.0214/0.0460

[a]$R_1 = \sum||F_o| - |F_c||/\sum|F_o|$. [b]$wR_2 = [\sum w(F_o^2 - F_c^2)^2/\sum w(F_o^2)^2]^{1/2}$.

Table S3. Selected bond lengths (Å) and bond angles (°) for $[DMPZ]MnCl_4$.

Mn1-Cl1	2.4080(6)	Mn1-Cl3	2.3366(4)
Mn1-Cl2	2.3984(6)	Mn1-Cl3^1	2.3366(4)
Cl3^1-Mn1-Cl3	120.77(2)	Cl3-Mn1-Cl1	105.226(13)
Cl3-Mn1-Cl2	110.570(13)	Cl3^1-Mn1-Cl1	105.226(13)
Cl3^1-Mn1-Cl2	110.571(12)	Cl2-Mn1-Cl1	102.58(2)

Table S4. Hydrogen bonds data for $[DMPZ]MnCl_4$.

D-H···A	d(D-H)	d(H···A)	d(D···A)	<(DHA)
N(1)-H(1)···Cl(1)	0.98	2.68	3.3960(12)	131
N(1)-H(1D)···Cl(2)	0.98	2.60	3.3934(12)	138
C(1)-H(1A)···Cl(3)	0.97	2.68	3.5804(14)	155
C(3)-H(3A)···Cl(3)	0.97	2.80	3.6476(15)	147

Table S5. Crystal Data and Structural Refinements for $[DMPZ]_2(MnCl_6)(MnCl_4)\cdot(H_2O)_2$.

Compound	$[DMPZ]_2(MnCl_6)(MnCl_4)\cdot(H_2O)_2$
chemical formula	$C_{24}H_{67.4}N_8O_{1.7}Mn_3Cl_{14}$
fw	1156.58
Space group	C2/c
a/Å	12.5515(15)
*b*Å	14.5375(18)
c/Å	27.789(3)
α/°	90.00
β/°	90.00
γ/°	91.00
V(Å^3)	5069.8(10)
Dcalcd (g·cm^{-3})	1.515
Temp (K)	273.15
μ (mm^{-1})	1.506
F (000)	2376.0
Reflections collected	26687
Unique reflections	6223
GOF on F^2	1.025
[a]R_1,wR_2 ($I > 2\sigma(I)$)	0.0310/0.0719
[b]R_1,wR_2 (all data)	0.0396/0.0763

[a]$R_1 = \sum||F_o| - |F_c||/\sum|F_o|$. [b]$wR_2 = [\sum w(F_o^2 - F_c^2)^2/\sum w(F_o^2)^2]^{1/2}$.

Table S6. Selected bond lengths (Å) and bond angles (°) for $[DMPZ]_2(MnCl_6)(MnCl_4)\cdot(H_2O)_2$.

Mn1-Cl3[1]	2.6248(5)	Mn1-Cl2[1]	2.4930(5)
Mn1-Cl3	2.6243(6)	Mn2-Cl7	2.3668(7)
Mn1-Cl1	2.5885(5)	Mn2-Cl4	2.3807(7)
Mn1-Cl1[1]	2.5883(5)	Mn2-Cl6	2.3494(6)
Mn1-Cl2	2.4926(5)	Mn2-Cl5	2.3287(7)
Cl3[1]-Mn1-Cl3	90.38(2)	Cl3[1]-Mn1-Cl2[1]	91.984(16)
Cl3[1]-Mn1-Cl1	90.555(17)	Cl3-Mn1-Cl2[1]	86.277(16)
Cl3-Mn1-Cl1	178.929(17)	Cl1-Mn1-Cl2[1]	94.219(16)
Cl3[1]-Mn1-Cl1[1]	178.939(17)	Cl1[1]-Mn1-Cl2[1]	87.546(16)
Cl3-Mn1-Cl1[1]	90.542(17)	Cl2-Mn1-Cl2[1]	179.53(2)
Cl1-Mn1-Cl1[1]	88.53(2)	Cl7-Mn2-Cl4	100.90(3)
Cl3[1]-Mn1-Cl2	87.684(16)	Cl7-Mn2-Cl6	104.42(3)
Cl3-Mn1-Cl2	93.394(16)	Cl5-Mn2-Cl6	113.32(2)
Cl1-Mn1-Cl2	86.115(16)	Cl7-Mn2-Cl5	118.32(3)
Cl1[1]-Mn1-Cl2	92.791(16)	Cl4-Mn2-Cl5	109.27(3)
Cl6-Mn2-Cl4	109.76(3)		

[1]1-X,+Y,1/2-Z

Table S7. Hydrogen bonds data for $[DMPZ]_2(MnCl_6)(MnCl_4)\cdot(H_2O)_2$.

D-H···A	d(D-H)	d(H···A)	d(D···A)	<(DHA)
N(1)-H(1)···Cl(4)	0.98	2.63	3.3193(18)	127
N(1)-H(1)···Cl(7)	0.98	2.60	3.4353(18)	143
O(1)-H(1D)···Cl(5)	0.87	2.54	3.389(2)	167
O(1)-H(1E)···Cl(2)	0.85	2.32	3.123(2)	157
N(2)-H(2)···Cl(3)	0.98	2.46	3.2737(18)	141
N(2)-H(2)···O(1)	0.98	2.19	2.867(3)	125
N(3)-H(3)···Cl(3)	0.98	2.73	3.4738(18)	133
N(3)-H(3)···Cl(2)	0.98	2.34	3.1462(17)	139
N(4)-H(4)···Cl(1)	0.98	2.70	3.4045(17)	129
N(4)-H(4)···Cl(2)	0.98	2.32	3.0971(16)	136
C(2)-H(2B)···Cl(7)	0.97	2.72	3.631(2)	157
C(4)-H(4A)···O(1)	0.97	2.44	2.914(3)	110
C(4)-H(4A)···Cl(4)	0.97	2.81	3.676(2)	149
C(4)-H(4B)···Cl(6)	0.97	2.80	3.482(2)	128
C(5)-H(5B)···Cl(1)	0.97	2.81	3.687(2)	151
C(8)-H(8A)···Cl(1)	0.97	2.70	3.642(2)	160
C(9)-H(9A)···Cl(2)	0.97	2.81	3.502(2)	129

Notes and references

1. F. Zhang, W. Liang, L. Wang, Z. Ma, X. Ji, M. Wang, Y. Wang, X. Chen, D. Wu, X. Li, Y. Zhang, C. Shan, Z. Shi, *Adv. Funct. Mater.* 2021, **31**, 2105771.
2. L. Zhou, J. F. Liao, Z. G. Huang, J. H. Wei, X. D. Wang, W. G. Li, H.Y. Chen, D. B. Kuang, C. Y. Su, *Angew. Chem. Int. Ed.* 2019, **58**, 5277-5281.
3. Z. Wang, Z. Zhang, L. Tao, N. Shen, B. Hu, L. Gong, J. Li, X. Chen, X. Huang, *Angew. Chem. Int. Ed.* 2019, **58**, 9974-9978.
4. M. E. Sun, Y. Li, X. Y. Dong, S. Q. Zang, *Chem. Sci.* 2019, **10**, 3836.
5. H. L. Liu, H. Y. Ru, M. E. Sun, Z. Y. Wang, S. Q. Zang, *Adv. Opt. Mater.* 2022, **10**, 2101700.
6. L. Gong , F. Huang, Z. Zhang, Y. Zhong, J. Jin, K. Z. Du, X. Huang, *Chem. Eur. J.* 2021, **424**, 130544.
7. J. Wu, Y. Guo, J. L. Qi, W. D. Yao, S. X. Yu, W. Liu, S. P. Guo, *Angew. Chem. Int. Ed.* 2023, **62**, e202301937.
8. X. Li, C. Peng, Y. Xiao, D. Xue, B. Luo, and X. C. Huang, *J. Phys. Chem. C.* 2021, **125**, 25112−25118.
9. H. Xiao, P. Dang, X. Yun, G. Li, Y. Wei, Y. Wei, X. Xiao, Y. Zhao, M. S. Molokeev, Z. Cheng, J. Lin, *Angew. Chem. Int. Ed.* 2021, **60**, 3699-3707.
10. Q. Kong, B. Yang, J. Chen, R. Zhang, S. Liu, D. Zheng, H. Zhang, Q. Liu, Y. Wang, K. Han, *Angew. Chem. Int. Ed.* 2021, 60, 19653-19659.
11. Z. Zhang, Y. Lin, J. Jin, L. Gong, Y. Peng, Y. Song, N. Shen, Z. Wang, K. Du, X. Huang, *Angew. Chem. Int. Ed.* 2021, **60**, 23373-23379.